BIOLOGY OF REPRODUCTION **72,** 879–889 (2005)
Published online before print 8 December 2004.
DOI 10.1095/biolreprod.104.033753

The Mouse Germ-Cell-Specific Leucine-Rich Repeat Protein NALP14: A Member of the NACHT Nucleoside Triphosphatase Family[1]

Michiharu Horikawa,[3] Nikki J. Kirkman, Kelley E. Mayo,[4] Sabine M. Mulders,[5] Jian Zhou,[6] Carolyn A. Bondy,[6] Sheau-Yu Teddy Hsu,[7] Gretchen J. King, and Eli Y. Adashi[2]

Division of Reproductive Sciences, Department of Obstetrics and Gynecology, University of Utah Health Sciences Center, Salt Lake City, Utah 84112

ABSTRACT

Microscopy of sectioned neonatal mouse ovaries established the predominance of primordial follicles in Day 3 samples and the predominance of primary follicles by Day 8. To identify genetic determinants of the primordial to primary follicle transition, the transcriptome of Day 1 or Day 3 mouse ovaries was contrasted by differential display with that of Day 8 ovaries. This manuscript examines one of the up-regulated genes, the novel *Nalp14* gene, whose transcript displayed 18- and 127-fold increments from Day 1 to Days 3 and 8, respectively. First noted by in situ hybridization in oocytes encased by primary follicles, *Nalp14* transcripts were continuously expressed through the preovulatory stage. The transcripts declined when meiotic maturation resumed, and they were markedly diminished by the 2-cell embryo stage. The corresponding 3281-base pair, full-length cDNA coded for a 993 residue/104.6-kDa germ cell-specific protein. A member of the multifunctional NACHT NTPase family, the NALP14 protein featured 14 iterations of the leucine-rich-repeat domain, a region implicated in protein-protein interaction. Protein BLAST analysis of the NALP14 sequence revealed 2 previously reported germ cell-specific homologs (i.e., MATER [Maternal Antigen That Embryos Require], RNH2 [RiboNuclease/Angiogenin Inhibitor 2], and NALP4c). The structural attributes, expression pattern, and cellular localization of MATER and RNH2 largely conformed to those reported for NALP14.

developmental biology, germ cell, leucine-rich repeat, meiosis, NACHT, oocyte, ovary, primary follicles

INTRODUCTION

The primordial follicle, home to a tetraploid, G_2-arrested oocyte, constitutes the resting, nongrowing, life-time germ-cell pool [1]. Arrested in prophase of meiosis I, the oocyte of the primordial follicle, encased by a single layer of flattened pregranulosa cells, remains transcriptionally and translationally quiescent until such time that its host follicle is recruited into the growing follicular pool [2]. The signal that initiates the growth of the primordial follicle, which is of critical importance to early folliculogenesis, remains unknown.

It was the purpose of this study to identify the proteins expressed during the transition from primordial follicle to primary ovarian follicle. Specifically, efforts were undertaken to identify those genes and proteins that may be concerned with this transformation. To date, genes that may partake in the primordial-to-primary follicular transition remain largely elusive. Among somatic genes, the *Kit* ligand, *Amh* (i.e., anti-Mullerian hormone) and the activins have been implicated [3–5]. Among germ cell genes, however, no viable candidates can be identified at this time.

This communication focuses on a single, novel mouse transcript/protein uncovered by differential display technology, designated NALP14, which is an orthologue to the previously identified human NALP14 (GenBank accession number NM_176822). We also report on 2 related oocytic proteins of the leucine-rich-repeat replete NACHT (NAIP, neuronal apoptosis inhibitory protein; CIITA, MHC class II transcription activator; HET-E, incompatibility locus protein from *Podospora anserina*; and TP1, telomerase-associated protein) [6] NTPase family, which at present, in the mouse, comprises a total of 3 members [7].

MATERIALS AND METHODS

Animals

Female C57BL/6J mice were purchased from Jackson Laboratories (Bar Harbor, ME). When they arrived they were 19 days of age, and were initially quarantined for 3 days at the University of Utah Animal Resources Center. The latter adheres to the guidelines outlined by The Animal Welfare Act and to institutional animal care and use committee protocols.

Collection of Oocytes and Embryos

C57BL/6J female mice 3–5 wk of age were injected with 10 IU of eCG (Calbiochem-Novabiochem Corp.). Germinal vesicle (GV)-stage oocytes were collected by puncturing mouse ovarian follicles 44–48 h after the injection of eCG. Some eCG-primed mice were injected with 10 IU of hCG (Sigma, St. Louis, MO). Unfertilized metaphase II (MII) oocytes were collected at 16 h post-hCG from the incised oviductal ampulae of superovulated/unmated female mice. The adherent cumulus cells were removed from cumulus-oocyte complexes by digestion with 1% hyaluronidase (Sigma). Fertilized 2-cell embryos were obtained 41–42 h post-hCG by flushing the oviducts of superovulated/mated female mice. Three 8-

[1]E.Y.A. was supported in part by grants HD30288 and HD37845 from the National Institutes of Health.
[2]Correspondence: Eli Y. Adashi, Department of Obstetrics and Gynecology, University of Utah Health Sciences Center, Salt Lake City, UT 84112. FAX: 801 585 9295; e-mail: eadashi@hsc.utah.edu
[3]Current address: Department of Obstetrics and Gynecology, Asahikawa Medical College, Midorigaoka Higashi 2-1-1-1, Asahikawa 078-8510, Japan.
[4]Current address: Department of Biochemistry, Molecular Biology and Cell Biology, Northwestern University, 2205 Tech Drive, Evanston, IL 60208.
[5]Current address: Organon, Kloosterstraat 6, 5349 AB Oss, The Netherlands.
[6]Current address: Developmental Endocrinology Branch, National Institute of Child Health and Human Development, National Institutes of Health, Bethesda, MD.
[7]Current address: Department of Gynecology and Obstetrics, Stanford University School of Medicine, 300 Pasteur Drive, Room A344, Stanford, CA 4305-5317.

Received: 19 July 2004.
First decision: 5 September 2004.
Accepted: 25 October 2004.

ISSN: 0006-3363. http://www.biolreprod.org

cell-stage embryos were collected 60–72 h post-hCG treatment by flushing the oviducts of superovulated/mated female mice. Blastocyst-stage embryos were isolated beginning with 2-cell-stage embryos for 96 h post-hCG treatment. The Hepes-buffered Dulbecco modified Eagle medium was supplemented with Earle balanced salt solution, essential amino acids (Gibco-BRL), 110 mg/L sodium pyruvate, 75 mg/L penicillin G, 50 mg/L streptomycin, and 0.5% BSA. Embryo cultures were carried out at 37°C under 5% CO_2 and air.

Isolation of Total RNA

Total RNA was isolated from the following nonovarian tissues of immature 25-day-old C57BL/6J mice: brain, thalamus, heart, kidney, liver, testis, and lung. Total RNA was also isolated from the ovaries of mice at Postnatal Days 1, 3, 8, and 10 and at 2, 3, 4, and 76 wk. Total RNA was isolated with the StrataPrep Total RNA Microprep Kit (Stratagene Corp.) according to the manufacturer's directions.

Differential Display

Differential display was performed with the Delta DD Kit (Clontech). Total RNA (2.0 μg) isolated from whole ovaries at Postnatal Days 1, 3, and 8 was treated with DNase I (Roche Applied Science) to eliminate potential contamination with genomic DNA and then reverse-transcribed by using each of three 1-base-anchored oligo-dT primers. First-strand cDNAs were amplified by polymerase chain reaction (PCR; 28 cycles) with 1 of 10 arbitrary primers (provided in the kit) and three 1-base anchoring primers. All amplified cDNAs were radiolabeled with [^{33}P]dATP (1000–3000 Ci/mM; ICN Pharmaceuticals). The resultant radiolabeled amplicons were electrophoresed on 6% polyacrylamide sequencing gels. After autoradiography, the bands were visually assessed. Differentially expressed bands (as confirmed in duplicate PCR amplification) were excised from the gel, reamplified by PCR, and cloned for sequencing.

Cloning and Sequencing of Complementary DNAs

Differentially displayed bands were purified with a Gel Extraction Kit (Qiagen Genomics, Inc.) and ligated into the pGEM-T Easy vector (Promega, Madison, WI). The latter was in turn transformed into the *Escherichia coli* strain XL-2 Blue (Stratagene), the resultant plasmids were purified by using miniprep kits (Qiagen), and the purified plasmids were sequenced with T7 or SP6 primers by ABI 377 automated sequencers (Perkin-Elmer Corp.), at the DNA sequencing core facility at the University of Utah Health Sciences Center. The sequence data were analyzed using the Basic Local Alignment Search Tool (BLAST) for homology to previously characterized genes deposited in the databases at the National Center for Biotechnology Informatics.

Rapid Amplification of cDNA Ends

To extend the 5′ and 3′ ends of the cDNA in question, rapid amplification of cDNA ends (RACE) was performed by using the SMART RACE cDNA Amplification Kit (Clontech). Complementary DNA was synthesized from total ovarian RNA of 4-wk-old mice as recommended by the manufacturer. The resultant amplicons were separated by electrophoresis on an agarose gel, extracted with the Qiagen Gel Extraction Kit (Qiagen), ligated into a pGEM-T Easy vector (Promega), and sequenced as described above.

Quantitative (Real-Time) PCR

LightCycler PCR (Roche Molecular Biochemicals) was carried out in a 20-μl reaction volume by rapid cycling in glass capillaries. Relevant reagents included Taq DNA polymerase (Promega), 10× PCR buffer with 3 mM Mg^{2+} (Idaho Technology), nucleotides (Idaho Technology), template DNA, primers (0.5 μM each), and SYBR green I dye (Molecular Probes Inc.). Primer pairs were as follows: 1) *Nalp14* forward, ATCCTGCGACCTGAATGTAGCC; reverse, ATCCCCACAAGCCTTA CTCGTG; 2) *Nalp5* (hereafter referred to as *Mater*) forward, GTGGAC AGAGAAGAGCAGTTTGGC; reverse, TAGAGGGGGGACACAACCA TTGAC; and 3) *Rnh2 (Nalp4c)* forward, ACTTGGACCTCAACCTCAC ATTCC; reverse, CAGAGAACCTTCAGCCCTTCATCC. SYBR green I fluorescence was detected at the end of each elongation cycle to monitor the amount of PCR product formed during that cycle. After the conclusion of the amplification process, a final melting curve was recorded by cooling the sample to 65°C at a rate of 20°C/sec, maintaining the reaction at 65°C for 15 sec, followed by heating slowly at 0.2°C/sec up to 95°C with continuous measurement of fluorescence. At the end of each run, a melting curve analysis of the amplification reaction was performed to increase the specificity and sensitivity of SYBR green I detection. The fluorescence signal (F) was plotted against temperature (T) to produce melting curves for each sample (F vs. T). Melting curves were then converted to melting peaks by plotting the negative derivative of the fluorescence with respect to fluorescence against temperature (−df/dT vs. T). Thus, each specific PCR product should produce an amplicon-specific signal that results in a product-specific melting peak.

In Situ Hybridization

The *Nalp14* cDNA ligated into the vector pGEM-T EASY was used to generate RNA probes for in situ hybridization. A digoxigenin (DIG)-labeled antisense RNA probe, driven by a T7 RNA polymerase, was obtained from an *Nde*I-digested template by using a DIG RNA labeling kit (Boehringer-Mannheim). A sense probe (negative control) was prepared by using an *Nco*I-digested template, SP6 RNA polymerase, and the DIG RNA labeling kit. Slide-mounted ovarian sections were hybridized with a 1:100 dilution of the antisense or sense probe for 16 h at 55°C in 50% formamide, 4× SSC, 1× Denhardt solution, 10% dextran sulfate, 0.25 mg/ml yeast tRNA, and 0.5 mg/ml salmon sperm DNA. After hybridization, the slides were washed in 50% formamide/2× SSC for 20 min at 50°C, and the hybridized probe was detected with an alkaline phosphatase-conjugated anti-DIG antibody (Boehringer-Mannheim). The alkaline phosphatase reaction was developed with 5-bromo-4-chloro-3-indolyl phosphate and with nitroblue tetrazolium (Boehringer-Mannheim).

RNA probes labeled with [^{35}S] were synthesized to a specific activity of about 2×10^8 dpm/μg by using a previously described protocol [8]. The sections were fixed; soaked for 10 min in 0.25% acetic anhydride, 0.1 M triethanolamine hydrochloride, and 0.9% NaCl; washed; and dehydrated. The [^{35}S]-labeled probes (107 cpm/ml) were added to a hybridization buffer composed of 50% formamide, 0.3 M NaCl, 10 mM Tris HCl pH 8, 1 mM EDTA, 1× Denhardt solution, 10% dextran sulfate, 10 mM dithiothreitol, and 750 μg yeast transfer RNA/ml. Coverslips were placed over the sections and the slides were incubated in humidified chambers overnight (14 h) at 47°C. Slides were washed several times in 4× SSC (NaCl and sodium citrate, Biosource International Inc.) to remove the coverslips and the hybridization buffer. Sections were then treated with ribonuclease A (20 μg/ml) for 60 min at room temperature, followed by washing in 0.5× SSC at 65°C for 30 min and 0.1× SSC at 65°C for 1 h. Slides were air-dried and apposed to Hyperfilm-beta Max (Amersham Biosciences Corp.) for 2 days and then dipped in Kodak NTB2 nuclear emulsion, stored with desiccant at 4°C for 6 days, developed, and stained with Mayer hematoxylin-eosin for microscopic evaluation. The specificity of the in situ hybridization results was confirmed by the observation that the antisense probes yielded a unique spatio-temporal pattern in the ovary, whereas the sense probe produced a diffuse, very low level radioactive signal.

Generation of a Specific Polyclonal Antibody Against the Mouse NALP14 Protein

An anti-NALP14 serum, raised in rabbits by Bethyl Laboratories Inc. against a 15-mer peptide (YQQNLRKHELTREDI) at the carboxy tail of the NACHT domain (residues 345–360), was affinity-purified. The antigen sequence did not overlap with the sequences of MATER (i.e., Maternal Antigen That Embryos Require) and RNH2 (i.e., RiboNuclease/Angiogenin Inhibitor 2).

Western Blot Analysis of NALP14 of the Mouse Ovary and Testis

Whole ovarian and testicular material from 28-day-old mice was homogenized in 40 mM Tris-HCl pH 7.5, 150 mM NaCl, and a protease inhibitor cocktail (Sigma). Tissue extracts were initially centrifuged at 20 000 × *g* for 15 min, the corresponding supernatants were removed, protein kinase inhibitor (Sigma) was added, and the mixture was stored at −80°C. Thereafter, tissue extracts (25 μg) were loaded onto and resolved on a 10% SDS-PAGE gel, followed by blotting onto nitrocellulose membranes. The blots were subsequently blocked with 5% nonfat dry milk in 10 mM Tris, 150 mM NaCl, 0.05% Tween-20 (TTBS), for 1–2 h before incubation with 3.4 mg/L of the rabbit anti-mouse NALP14 antibody. The secondary antibody, conjugated to peroxidase (Amersham Pharmacia), was diluted 1/5000. The signal was detected by means of the enhanced chemiluminescence system (Amersham Pharmacia). For the purpose of peptide-mediated immunoneutralization of the NALP14 antibody, the latter was

incubated overnight in 5 ml of PBS at 4°C with 17.0 mg/L of the synthetic NALP14 peptide (LYQQNLRKHELTREDI).

Morphology and Immunohistochemistry

Ovaries were surgically removed, fixed for 4 h in 10% neutral buffered formalin at room temperature, embedded in paraffin wax to maximize morphologic integrity, and sectioned (3-μm intervals). Tissue sections were deparaffinized and rehydrated through xylene and a graded alcohol series, and stained with hematoxylin-eosin using standard protocols. Immunostaining was performed with the Ventana automated IHC staining system (Ventana Medical Systems Inc.) with a diaminobenzidine kit. Sections were incubated for 32 min at a 1:160 dilution of the affinity-purified primary (rabbit) antibody against NALP14. After washing, the slides were reincubated for 8 min with a 1:300 dilution of a secondary antibody against rabbit immunoglobulin G (Sigma). The resultant sections were counterstained lightly with hematoxylin. Negative controls consisted of identical reactions with the omission of the primary antibody.

RESULTS

Postnatal Follicular Ontogeny of the Mouse Ovary

To experimentally establish the optimal parameters for the differential screening procedure that was designed to compare and contrast primary with primordial follicles, mouse ovaries were collected daily between Day 1 (the day of birth) and Day 10 of life. Oogonia lacking an organized layer of surrounding granulosa cells were referred to as such. Primordial follicles were defined as the unit consisting of a 15- to 20-μm GV-stage oocyte surrounded by a single layer of flattened (noncuboidal) pregranulosa cell. Follicles featuring GV-stage oocytes—those surrounded by a mixture of flattened and cuboidal follicular cells—were categorized as intermediate. Primary follicles in turn were identified as those containing a growing (~30 μm) oocyte surrounded by a single layer of cuboidal granulosa cells. Finally, secondary preantral follicles consisted of a growing (~50 μm) oocyte encased by 2 or more layers of granulosa cells. No developmental stages beyond the secondary preantral follicle were apparent during the time frame examined. Analysis of the relative representation of the various follicular stages throughout the first 10 days of life was assessed in at least 4 sections from each of 8 mice. Oogonia proved predominant in Day 1 samples (92.2% of the germ cell complement). By Postnatal Day 3, half of the germ cells had been incorporated into primordial follicles. Progression to the intermediate follicle stage was barely evident by Day 3. However, from Day 4 to Day 10, intermediate follicles constituted a steady representation of 7%–18% of the total germ cell complement. Progression to primary follicles, first evident on Day 5, increased progressively after Day 6. A few secondary follicles, first noted on Days 7 and 8, assumed increasing prevalence on Days 9 and 10. Given the above, the Day 3 ovary was selected as optimal for the isolation of primordial follicles in that the relative representation of the primordial follicle population may have been maximized. A Day 4 selection in turn would have to contend with the potentially confounding influence of the now emerging intermediate-stage follicles. The Day 8 ovary was selected as optimal for the isolation of primary follicles, thereby avoiding the subsequent increase in secondary stage preantral follicles. The dominant distinction between Day 8 and Day 3 ovaries proved to be the presence of primary follicles in the former. In contrast, both Day 3 and Day 8 ovaries were comparably endowed with primordial follicles. A numerical tally of the germ cell development at Days 1–10 after birth and representative micrographs from Days 1, 3, 5, and 8 are shown in Figure 1 and Table 1.

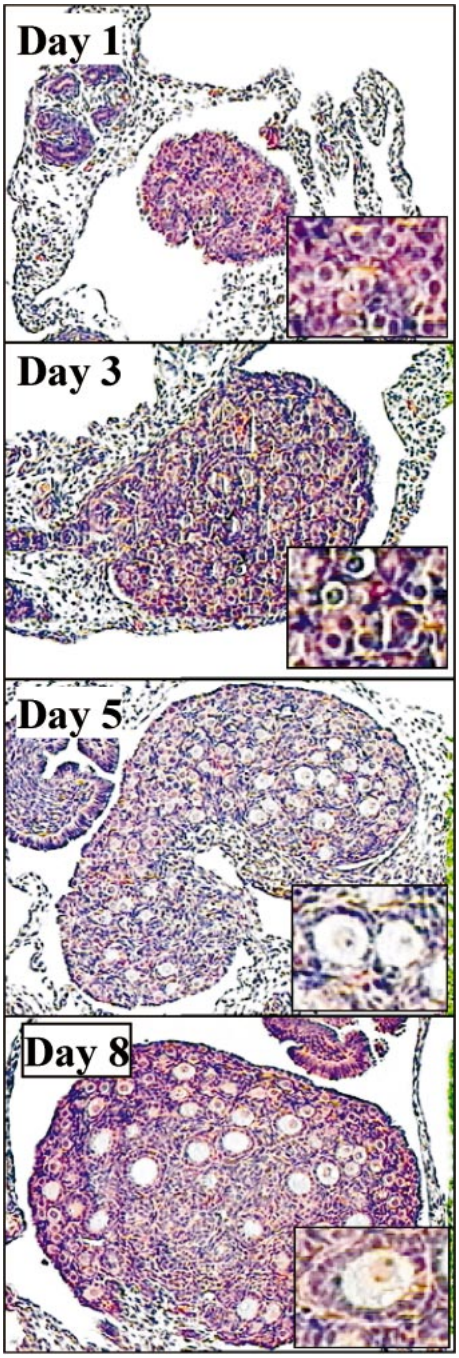

FIG. 1. Follicular ontogeny of the neonatal mouse ovary: morphology. Ovaries were removed daily from newborn female C57BL/6J mice between Day 1 (the day of birth) and Day 10 of life. Each daily panel contains a low-magnification (×100) view and a lower, right-hand corner, higher-magnification (~×400) insert highlighting the oocytic/follicular developmental stage. Data were captured with a reverse-phase Olympus IX70 Microscope.

Differential Display Analysis of Day 1, 3, and 8 Transcriptomes of the Mouse Ovary

To identify potential genetic determinants of the transition from primordial to primary follicles, differential display was employed to categorize differentially expressed ovarian genes on Postnatal Days 1, 3, and 8. A Day 1 sample was included as a representative of an oogonia-dominant state. In all, 58 differentially expressed bands (i.e., differentially expressed in one of the days under

TABLE 1. Ovarian germ cell ontogeny.

Postnatal day	Oogonia n (%)	Primordial follicles n (%)	Intermediate follicles n (%)	Primary follicles n (%)	Secondary follicles n (%)
1	566 (92)	48 (8)	0	0	0
2	51 (86)	8 (14)	0	0	0
3	115 (48)	122 (51)	3 (1)	0	0
4	16 (8)	177 (83)	20 (9)	0	0
5	22 (4)	459 (78)	86 (15)	21 (4)	0
6	8 (6)	97 (75)	23 (18)	1 (1)	0
7	10 (2)	333 (79)	30 (7)	46 (11)	5 (1)
8	0	162 (66)	36 (15)	43 (17)	6 (2)
9	0	139 (58)	33 (14)	45 (19)	23 (10)
10	0	91 (49)	27 (15)	48 (26)	20 (11)

study), were visually identified (not shown). Of those, 32 bands represented an up-regulated pattern (Day 8 > Day 3 > Day 1), 24 bands represented a down-regulated pattern (Day 8 < Day 3 < Day 1), the remaining 2 bands being expressed solely on Day 3 (not shown). Differentially expressed bands were excised from the gel, reamplified by PCR, and sequenced. To confirm the differential ovarian expression of the cDNA sequences, quantitative, real-time reverse transcription (RT)-PCR (QRT-PCR) analysis was employed. Especially noteworthy from among the up-regulated gene candidates was band P3G2 (named for the corresponding primer pair designation). Of importance, QRT-PCR analysis of this transcript disclosed 18- and 127-fold increments (relative to Postnatal Day 1) on Postnatal Days 3 and 8, respectively (Fig. 2). Accordingly, we have cloned and characterized this potential determinant of the primordial-to-primary follicular transition.

Cloning of the Full-Length cDNA Corresponding to the Differentially Expressed P3G2 Band

Nucleotide analysis of the P3G2 sequence with the Basic Local Alignment Search Tool (BLAST) revealed significant identity (97%) to 192 base pairs (bp) (Fig. 3) at the 3′ end of a previously reported 1434-bp (putatively full-length) cDNA, derived from the adult testis and reported by the RIKEN Institute (Wako, Japan). For the purpose of this discussion, the latter cDNA will be referred to by its GenBank accession number, AK014932. Initial 5′ RACE, applied to AK014932 cDNA, relied on 3′-5′ 26-nt primers anchored at nucleotide 486 of the cDNA. This in turn was followed by repeat, and progressively 5′-oriented extensions, resulting in a 3281-bp full-length cDNA, the open reading frame component comprising 2979 bp (Fig. 3; GenBank accession number AC673647). The latter, the subject of this communication, was designated *Nalp14.*

Genomic Organization and Allelic Representation of the Nalp14 *Gene*

The mouse genomic database (Ensemble Mouse Genome Server, http://www.ensembl.org/Mus_musculus/blastview) was subjected to nucleotide BLAST analysis against the full-length sequence of the *Nalp14* cDNA. Note was made of a single, highly homologous match on chromosome 7. A more detailed analysis disclosed the *Nalp14* gene to consist of 11 exons and 10 introns over a 30-kilobase (kb) stretch (not shown). Analysis of the intron-exon junctions, established appropriate (AG-GT) splice sites in each case [9].

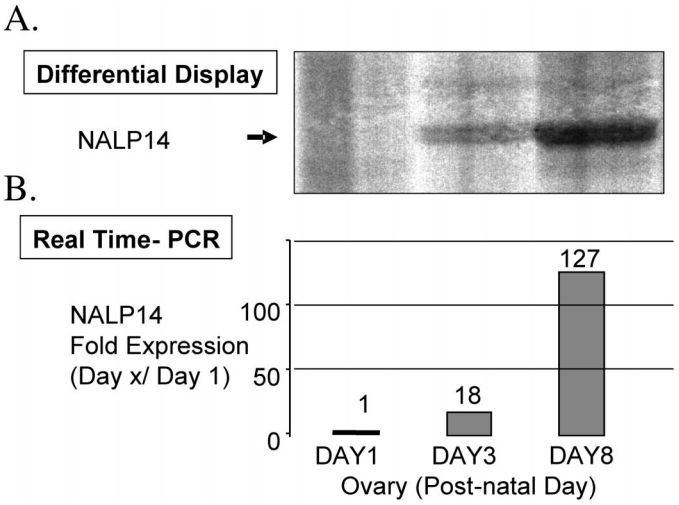

FIG. 2. Autoradiogram of differentially displayed/PCR-amplified *Nalp14* and QRT-PCR. **A**) Total RNA isolated from whole ovaries on Postnatal Days 1 (the day of birth), 3, and 8 was subjected to RT-PCR in the presence of [^{33}P-dATP] and the resulting radiolabeled amplicons were electrophoresed through 6% polyacrylamide gels and analyzed by autoradiography. **B**) Representation of the fold increase from Day 1 on Days 3 and 8 of *Nalp14* mRNA from one sample as assessed by QRT-PCR.

Initial Characterization of the NALP14 Transcript and Protein

Nucleotide BLAST analysis of the 3281-bp *Nalp14* cDNA sequence disclosed the 1183-bp segment at the 3′ end of *Nalp14* (including the 192-bp P3G2 fragment), to display 98% identity with the 1434-bp testicular AK014932 cDNA (Fig. 3). To confirm that the *Nalp14* cDNA was full length, mouse ovarian total RNA was subjected to Northern blot analysis, revealing a single band, approximately 3.3 kb in size, a size consistent with the presumptive full-length

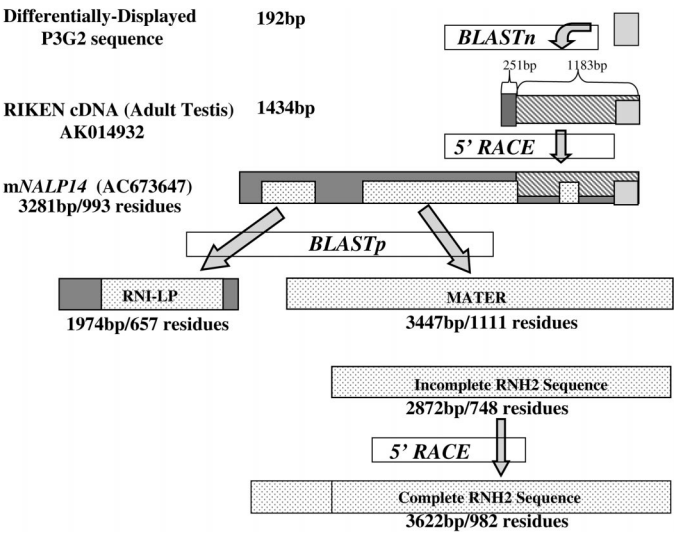

FIG. 3. Schematic Representation of the progression from the differentially displayed P3G2 band to the cloning of the full-length cDNAs of *Nalp14* and *Rnh2*. Nucleotide BLAST analysis of the P3G2 sequence revealed significant identity with the terminal 192 bp at the 3′ end of a previously reported AK014932 cDNA. The application of 5′ RACE to the latter yielded a putative, full-length cDNA of the *Nalp14* gene. Protein BLAST analysis of the latter disclosed variable identity with RNI-LP, the putative translated product of a known genomic sequence, with the previously described MATER protein and with the putative (in retrospect incomplete) RNH2 protein.

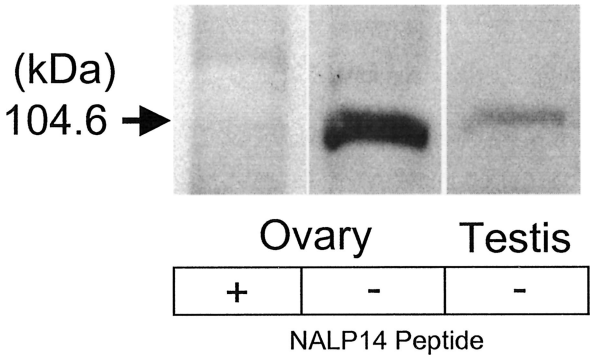

FIG. 4. Expression of the NALP14 gene and protein in the mouse ovary: Western blot analyses. Protein extracts (25 μg/lane) from adult ovary or testis were subjected to Western blot analysis. Specificity of the immunoreactive signal was assessed by preincubation of the primary anti-NALP14 antibody with the synthetically prepared, affinity-purified, 15-mer immunogenic peptide (YQQNLRKHELTREDI) (left lane).

Nalp14 cDNA (not shown). Western blot analysis (Fig. 4) in turn revealed the immunoreactive NALP14 protein to display a molecular mass of 104.6 kDa in both the ovary and the testis. The latter figure is in good agreement with the calculated theoretical molecular weight of 113 kDa (pI = 6). The specificity of the NALP14-directed antibody was confirmed by the elimination of ovarian NALP14 immunoreactivity following preincubation with non-rate-limiting amounts of the synthetic (15-mer) immunogenic NALP14 peptide.

The Germ Cell Family of Leucine-Rich-Repeat Replete NACHT NTPase: Tissue Specificity Postnatal and Perifertilization Ontogeny, and Germ Cell Specificity

Ovarian total RNA, testicular total RNA, and total RNA from a number of extragonadal tissues (brain, thymus, heart, lung, liver, pancreas, and kidney) were subjected to QRT-PCR analysis with specific primers corresponding to the *Nalp14*, *Mater*, and *Rnh2* cDNAs. As shown (Fig. 5A), transcripts corresponding to the *Nalp14* and *Rnh2* genes could be documented only in the ovary and the testis. Transcripts corresponding to the *Mater* gene were, in turn, further limited to the ovary.

Whole ovarian total RNA isolated on Days 1, 3, 5, 8, and 10, as well as in Weeks 2, 3, 4, and 76 of life, was subjected to QRT-PCR analysis. As shown (Fig. 5B), peak expression of *Mater* transcripts (like *Nalp14* transcripts), was noted on Day 8 of life. Peak expression of *Rnh2* transcripts in turn was somewhat delayed, becoming most evident at 2 wk of life. Of importance, none of the transcripts could be detected by 76 wk of life, a time characterized by an apparent, complete loss of oocytes in the C57BL/6J strain under study (not shown).

To evaluate the expression pattern of transcripts during perifertilization corresponding to genes of the germ cell family of leucine-rich-repeat (LRR) replete NACHT NTPases, total RNA was obtained from the GV-stage oocyte, the MII-stage oocyte, the 2-cell-stage embryo, 3- to 8-cell-stage embryos, and the blastocyst and subjected to QRT-PCR analysis. As shown (Fig. 5C), a precipitous, and indeed simultaneous decline in the steady state levels of all the transcripts under study was noted within the GV-to-MII transition. Although a modicum of these transcripts could still be documented in MII-stage oocytes, little or no expression could be detected beyond that point. Recently, a

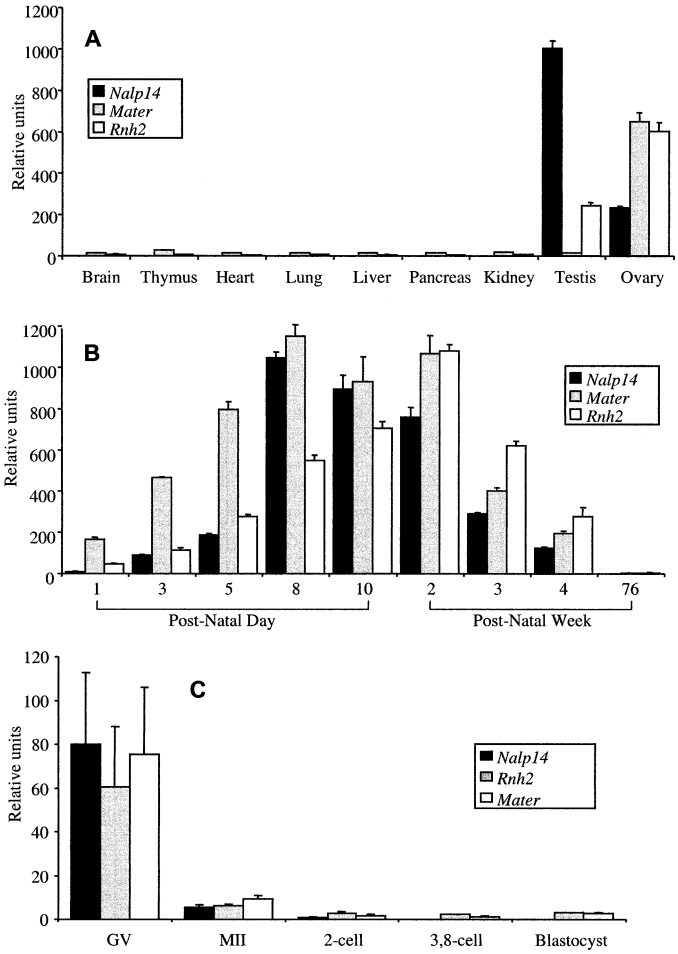

FIG. 5. Expression of transcripts corresponding to members of the germ cell family of LRR-replete NACHT NTPases: tissue specificity, postnatal and perifertilizational ontongeny. **A**) To evaluate the tissue-specific patterns of expression of the germ cell family of LRR-replete NACHT NTPases (*Nalp14, Mater,* and *Rnh2*), ovarian total RNA, testicular total RNA, and total RNA from a number of extragonadal tissues (brain, thymus, heart, lung, liver, pancreas, and kidney) were subjected to QRT-PCR analysis. **B**) To evaluate the postnatal ontogeny of the germ cell family of LRR-replete NACHT NTPases, whole ovarian total RNA isolated on Days 1, 3, 5, 8, and 10 of life, as well as in Weeks 2, 3, 4, and 76 of life, was subjected to QRT-PCR analysis with specific primers corresponding to the *Nalp14, Mater,* and *Rnh2* cDNAs. **C**) To evaluate the perifertilization expression pattern of transcripts corresponding to the germ cell family of LRR-replete NACHT NTPases genes, total RNA was isolated from GV-stage and MII-stage oocytes, from 2-cell and 3- to 8-cell stage embryos, and from a blastocyst. GV, germinal vesicle; MII, metaphase II-stage oocyte. Relative units represent the signal intensity relative to that of β-actin. The results represent the mean ± 2 SEM of 3 independent experiments.

sequence corresponding to *Nalp14* was found in mouse oocytes at 4–5 wk after birth [10].

Cellular Localization of Ovarian Transcripts Corresponding to Members of the Germ Cell Family of LRR-Replete NACHT NTPases: In Situ Hybridization

The cellular localization of *Nalp14* transcripts in the mouse ovary was established on Day 8, a time of peak *Nalp14* expression. The *Nalp14* transcripts were clearly noted by in situ hybridization in intermediary, primary, and secondary (but not primordial) follicles (Fig. 6).

To assess the cellular localization of transcripts corresponding to members of the germ cell family of LRR-replete NACHT NTPases within the ovary, frozen sections

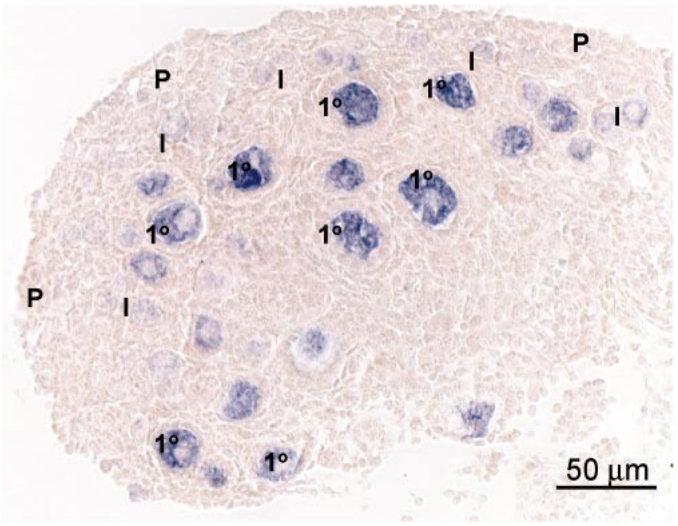

FIG. 6. The cellular localization of *Nalp14* transcripts in Day 8 ovaries was determined by in situ hybridization. *Nalp14* transcripts were clearly evident in Day 8 oocytes associated with intermediate (I) and primary (1°), but not primordial follicles. The corresponding sense preparations proved negative (not shown).

of ovarian material from 2-wk-old mice were subjected to in situ hybridization with riboprobes corresponding to the *Nalp14*, *Mater*, and *Rnh2* cDNAs. As shown (Fig. 7, A–R), none of the transcripts under study was detected in primordial follicles. Instead, expression was noted for all members of the LRR-replete NACHT NTPase family at the level of the primary and early preantral secondary follicle. These data suggest that *Rnh2* transcripts, similar to the *Mater* and *Nalp14* counterparts, are oocyte-specific and subject to a qualitatively comparable pattern of expression.

Cellular Localization of the NALP14 Protein in the Ovary and the Testis: Immunohistochemistry

The immunoreactive NALP14 protein studied in the adult ovary localized exclusively to the oocytic cytoplasm at all stages of follicular development, with the exception of the primordial follicle stage (Fig. 8, A–F). No signal was detected in granulosa or theca cells. In addition, note was made of NALP14 immunoreactivity in the germ cell elements of the seminiferous tubules of the adult testis (Fig. 8, G and H). No immunoreactivity was detected in the interstitial testicular spaces inclusive of Leydig cells. Ovarian and testicular sections stained in the absence of a primary antibody proved negative (not shown).

Characterization of the Germ Cell Family of LRR-Replete NACHT NTPases

Protein BLAST analysis of NALP14 (GenBank accession number AAT77542) disclosed 30% identity with the 1111-residue MATER (GenBank accession number Q9RIM5; Fig. 3), an established oocyte-specific (cytoplasmic) protein [11, 12]. The latter, like NALP14, was endowed with a 320-residue N-terminal-based NACHT NTPase domain and a C-terminal-based LRR domain (14 repeats), a structure known to be critical for protein-protein interactions [13].

Additionally, protein BLAST analysis uncovered 24% identity between NALP14 and the 748-residue RNH2 protein segment (Fig. 3), an X-linked gene product reported as highly expressed during spermatogenesis (GenBank accession number AK014932) [14]. In common with NALP14 and MATER, the C-terminal of the RNH2 protein sequence featured multiple repeats (13) of the LRR domain (Figs. 9 and 10). However, the 748-residue RNH2 protein segment (Fig. 3), unlike NALP14 or MATER, featured an incomplete NACHT NTPase region, lacking the P-loop domain (umbrella site Motif Scan, http://hits.isb-sib.ch/cgi-bin/PFSCAN_parser). A 5′ RACE reaction was carried out with mouse ovarian cDNA template extending the existing *Rnh2* cDNA by 750 bp to yield a 3622-bp full-length *Rnh2* cDNA with an open reading frame of 2947 bp (Fig. 3).

An additional, unheralded and common structural feature of the 3 proteins under study is the presence of a hydrophilic region proximal to the NACHT domain. The latter, assessed by the Kyte/Doolittle Hydrophilicity plot, revealed predominantly hydrophilic stretches of 80, 190, or 150 bp for NALP14, MATER, and RNH2, respectively (not shown).

Marked homology of the NACHT domains of NALP14, MATER, and RNH2 was noted in the 7 established motifs (I–VII) of the prototypic NACHT NTPases (Fig. 9). Especially striking homology was noted for the 8-residue P-loop signature, GXXGXGKS/T, a key NTP-binding component at the heart of motif I (also known as Walker A). In general, the third residue within the P-loop has been found to represent a small amino acid (A or P). The last residue of the P-loop, in turn, generally features a hydroxy residue (T or S). Also of note in the proximal (pre-P-loop) portion of the motif I sequence were 3 amino acids consisting of 2 consecutive hydrophobic residues (hh) followed by a third aliphatic residue represented by leucine (l). Further representation of periodically arranged 4 hydrophobic residues (leucine, arginine, methionine, tryptophan, and iso-leucine) is noted at the tail end (post-P-loop) of motif I.

A second component of the NACHT domain worthy of more detailed discussion is the Mg^{++} binding site (Walker B) contained within motif III. The 5 residues of the Mg^{++} binding site sequence, located at the C-terminal end of motif III (Fig. 9), comprised 4 consecutive hydrophobic residues (h) and a terminal D (asparatic acid) residue. Other conserved residues throughout the motif III region include a polar residue (p; Q, K, or D), several additional hydrophobic residues (h; V, F, I, L, or M), a single ''tiny'' residue (u; S, G, or N), a negatively charged residue (n; D or E), and a single ''big'' residue (b; E, D, or V).

Figure 9B illustrates the alignment of the LRR domains of NALP14, MATER, and RNH2. The general formula describing the LRR region of ribonuclease inhibitor (RI)-like proteins (e.g., NALP14), is represented by the sequence LxxLxLxxN/CxLxxxxoxxLxxoLxx, wherein o constitutes a nonpolar residue [15]. Proximally, each LRR domain consists of a 6-residue β-strand replete with 3 conserved leucines that on occasion are conservatively substituted by isoleucine, valine, phenylalanine, or methionine. The distal portion of the LRR domain in turn consists of a 20- to 23-residue α-helix, replete with up to 3 conserved leucines that on occasion are conservatively substituted by methionine, valine, iso-leucine, and phenylalanine. An exception to the preceding is the second LRR domain, for which only 2 conserved leucines were noted in the α-helical domain, an apparent deviation from the Kajava formula. Another departure from the Kajava formula is the apparent absence of a C/N at the 9th position in LRRs 1–3 otherwise present in LRR_4–LRR_{13} (vertical bar at the 9th residue of the LRR in Fig. 9B).

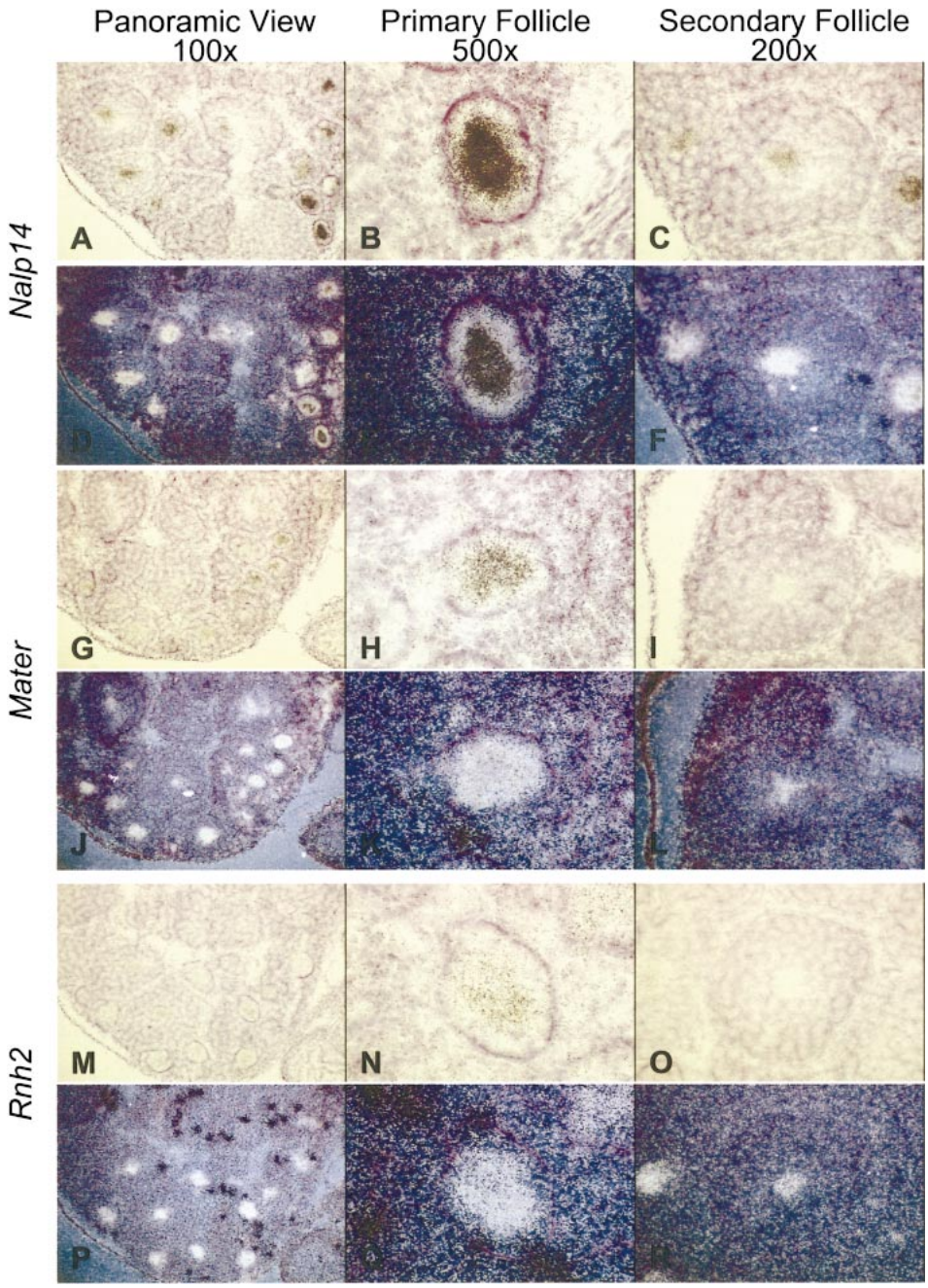

FIG. 7. To assess the cellular localization of transcripts corresponding to members of the germ cell family of LRR-replete NACHT NTPases within the ovary, frozen sections of ovarian material from 2 wk of life were subjected to in situ hybridization. *Nalp14:* brightfield (**A**–**C**), darkfield (**D**–**F**. *Mater:* brightfield (**G**–**I**), darkfield (**J**–**L**). *Rnh2:* brightfield (**M**–**O**), darkfield (**P**–**R**).

Three-Dimensional Structure of the LRR Domain of Members of the Germ Cell Family of LRR-Replete NACHT NTPases

Three-dimensional (3D) models of the LRR domain of members of the germ cell family of LRR-replete NACHT NTPases were generated using the Swiss Model Web site (http://www.expasy.org/swissmod/SWISS-MODEL.html). As shown (Fig. 10, A and B), the LRR domain of the NALP14 protein assumed a horseshoe, rather than a globular configuration. The resultant 3D model proved in keeping with that previously reported for the porcine ribonuclease inhibitor protein (ExPDB code 2BNH) the crystal structure of which has been solved (Fig. 10E) [16]. According to this model, the 14 β sheets of NALP14, likely fold to form an internal circle, the corresponding α helices constituting the external circumference of the horseshoe configuration. Also shown are the projected, largely homologous 3D structures of MATER (Fig. 10C) and RNH2 (Fig. 10D), replete with 14 and 12 β sheets, respectively.

DISCUSSION

Although this work focuses on a single derivative gene, *Nalp14*, a transcript displaying a 127-fold increase in its ovarian representation between Days 1 and 8 of life, the differential display analysis yielded an additional 57 genes whose expression was variably altered during this early phase of ovarian development (not shown). The 57 genes in question consisted of 7 of unknown function, 13 of known function, and 37 that were deemed novel (not shown). Consequently, much additional work will be required to characterize the function of the genes in question. As such, this repository of developmentally regulated genes likely accounts for a substantial representation of the total

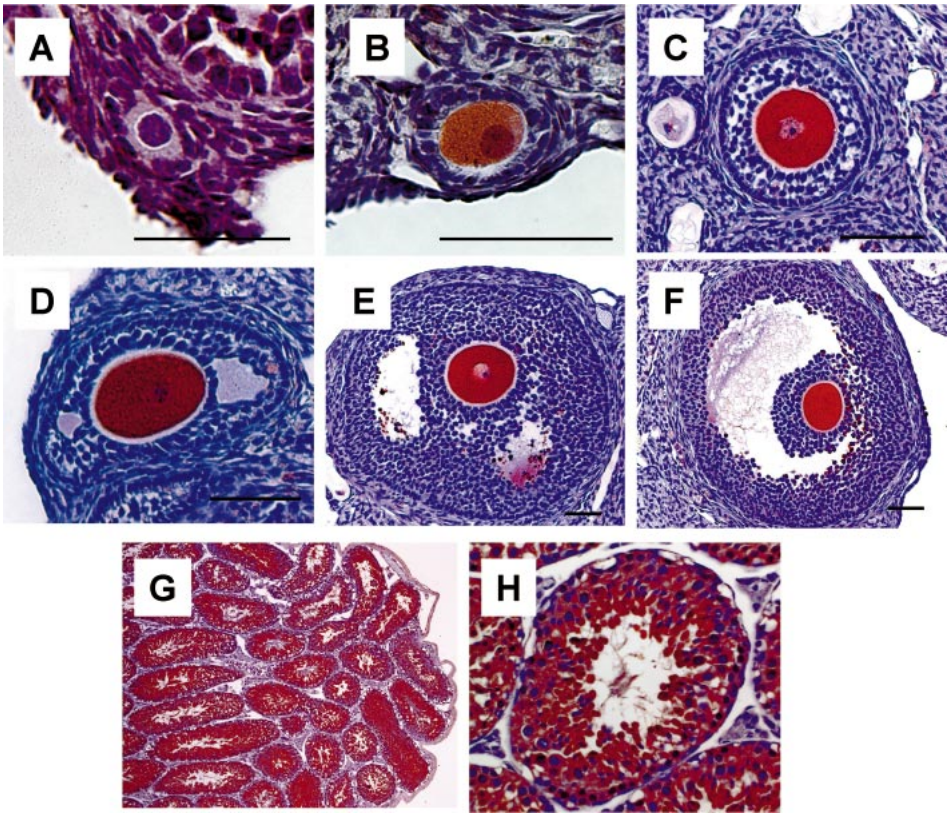

FIG. 8. To localize the NALP14 protein within the ovary and testis, 4-wk-old whole ovarian and testicular material were subjected to immunohistochemical studies. Ovarian sections: primordial follicle (**A**); primary follicle (**B**); preantral secondary follicle (**C**); early antral secondary follicle (**D**); late antral secondary follicle (**E**); preovulatory follicle (**F**); and (**G** and **H**) testicular sections, seminiferous tubules, graded magnification. Bar = 50 μm.

genetic program underlying the still enigmatic process of primordial follicle recruitment.

In the course of analyzing the primary structure of NALP14 and its oocytic family members, note was made of the existence of an N-terminal-based NACHT (NAIP, CIIA, HET-E, and TP1) domain [7, 9, 11, 14, 17]. This latter domain features an NTP (ATP/GTP) binding site (also known as P-loop, I, or Walker A motif) thereby imparting an NTPase function to this protein family. The P-loop, a glycine-rich region that typically forms a flexible loop between a β strand and an α helix, is the most conserved. In addition, the NACHT domain is home to a Mg^{++} binding site (Walker B or III motif), as well as to 5 additional structural motifs of unknown function. In the case of NALP14, the NACHT module is preceded at the N-terminus with a hydrophilic domain, the function of which remains uncertain. Conspicuously absent at the amino terminus were the commonly encountered CARD (Caspase Activation and Recruitment Domain), PAAD [Pyrin AIM (absent-in-melanoma), ASC (apoptosis-associated spec-like protein containing a CARD), and Death Domain-like] or BIR [Baculovirus Iap (inhibitor of apoptosis) Repeat] domains [18, 19]. Most vertebrate members of the NACHT family of proteins appear to be associated with programmed cell death or with the immune responses against pathogens. Special mention is made of CARD4 (a proapoptotic protein, [20]) and of NAIP (an antiapoptotic protein), both of which feature a C-terminus-based LRR domain. To the extent that the preceding structure-function relationship can be extrapolated, it is possible that NALP14 and members of its oocytic family may also be associated with programmed cell death in an NTP-dependent manner.

In the process of cloning the full-length *Nalp14* cDNA, initial nucleotide BLAST analysis disclosed significant, albeit incomplete identity, with an existing 1434-bp cDNA derived from the adult mouse testis RIKEN collection (Fig. 3). Although the bulk (1183 bp) of the 3′ end of the AK014932 cDNA in question proved to be 98% identical to the *Nalp14* sequence, the 5′ portion of the AK014932 cDNA (251 bp) proved entirely distinct from the *Nalp14* sequence. In that the cDNA featured multiple stop codons, the generation of a translated consensus open reading frame, and by extension, the execution of protein BLAST analysis was precluded. It is therefore tempting to speculate that the AK014932 cDNA may constitute a yet-to-be uncovered member of the germ cell family of LRR-replete NACHT NTPases, or an alternatively spliced version of *Nalp14*. One cannot, of course, preclude the possibility that the AK014932 cDNA constitutes a sequencing/computational artifact. Recent probing by RT-PCR with primers corresponding to the unique (non-*Nalp14*) 5′ 251-bp region of the AK014932 cDNA disclosed the presence of transcripts in the adult testis, but not in the ovary (not shown).

Further analysis of the sequence of the *Nalp14* cDNA revealed that components displayed 98% identity with *Rni-lp* (Ribonuclease Inhibitor-Like Protein). To determine whether *Rni-lp* cDNA is expressed in the mouse ovary, total RNA was subjected to RT-PCR analysis with a primer set common to both *Nalp14* and *Rni-lp*. It was reasoned that the size of the amplicon would identify the transcript in question (301 bp and 726 bp for *Rni-lp* and *Nalp14*, respectively). Whereas the *Nalp14* transcript was predictably amplified (not shown), no transcripts corresponding to the *Rni-lp* cDNA could be detected. It is thus concluded that the *Rni-lp* ''gene'' is not expressed in the adult mouse ovary.

Protein BLAST analysis of the NALP14 amino acid sequence also disclosed 30% identity with a known oocytic protein, MATER, uncovered by expression cloning. The latter was undertaken in an effort to uncover an ovarian

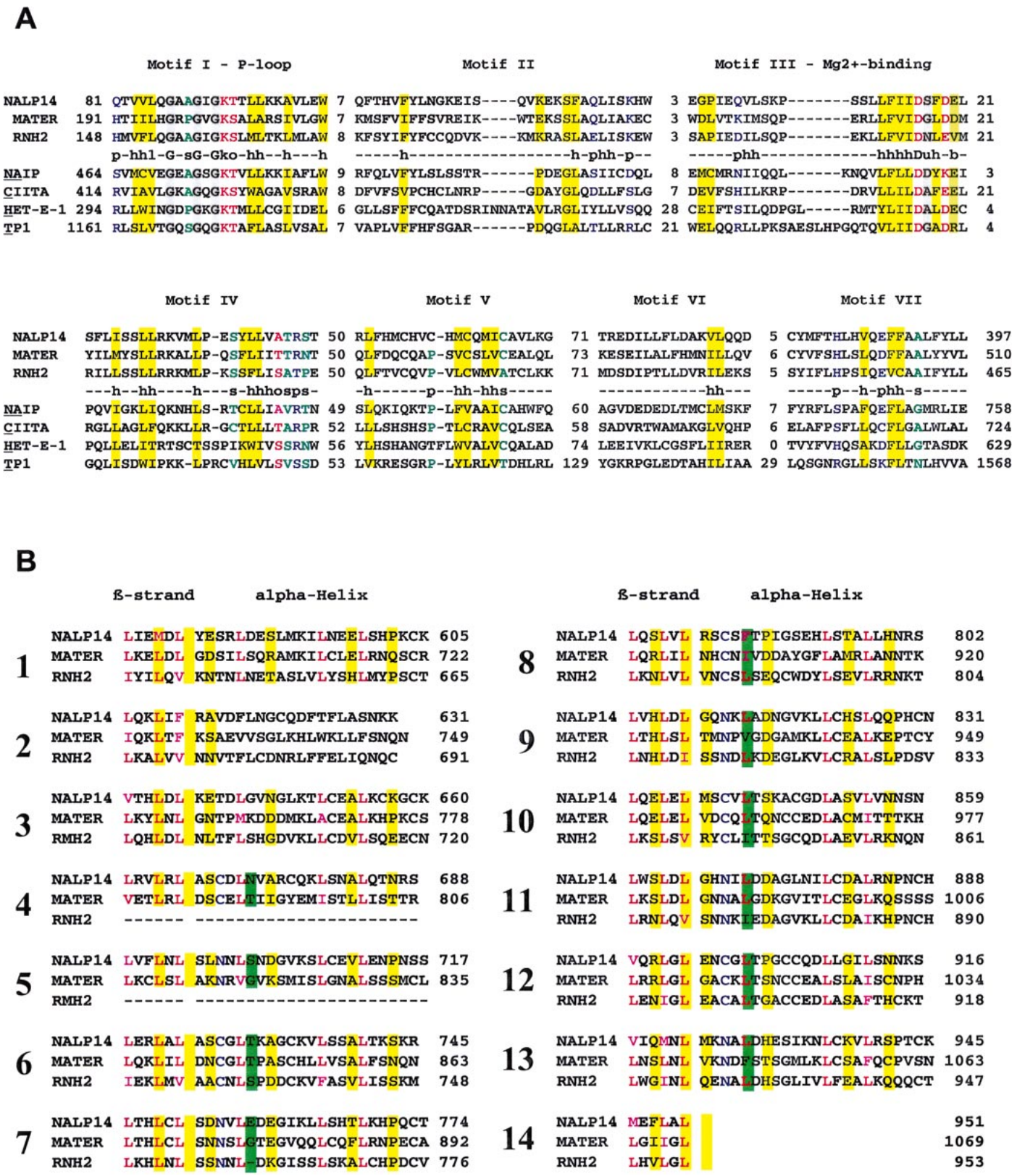

FIG. 9. The germ cell family of LRR-replete NACHT NTPases: the NACHT domain. **A**) Alignment of the amino acid sequences of the NACHT domains of NALP14, MATER, and RNH2. Reference alignment of the amino acid sequences of the prototypic NACHT proteins NAIP, CIITA, HET-E-1, and TP1 is likewise presented. MATER, Maternal Antigen That Embryos Require; Rnh2, RiboNuclease/Angiogenin Inhibitor 2; NACHT (amino terminus based domain), NAIP, CIITA, HET-E, and TP1; P-Loop, ATP/GTP-binding site (also known as Walker A; boxed residues); Mg^{++}-binding site (also known as Walker B; boxed residues); p, polar residue (D, E, H, K, N, Q, R, S, T); h, hydrophobic residue (A, C, F, I, L, M, V, W, Y); l, aliphatic residue (L, V, I); o, hydroxy residue (S, T); u, ''tiny'' residue (G, A, S); b, ''big'' residue (F, I, L, M, V, W, Y, K, R, E, Q); n, negatively charged residue (D, E) [15]. **B**) Alignment of the amino acid sequences of the LRR domains of NALP14, MATER, and RNH2. Arabic numerals 1–14 correspond to the number of internal β sheets. Only 13 LRRs have been aligned. Although LRR_{14} of NALP14 displays a β sheet, the existence of a corresponding α helix, comparable to helices 1–13 remains uncertain. The general formula describing the leucine repeat region of ribonuclease inhibitor-like proteins (e.g., NALP14), is represented by the sequence: LxxLxLxxN/CxLxxxxoxxLxxoLxx, wherein o constitutes a non-polar residue [15].

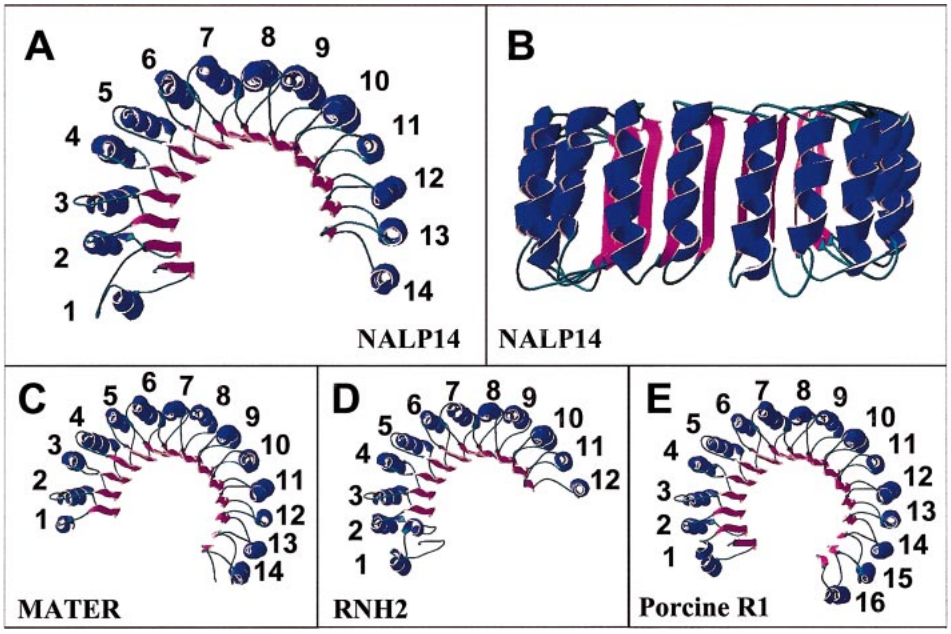

FIG. 10. Projected 3D depiction of the LRR region of NALP14, MATER, RNH2, and porcine ribonuclease inhibitor. Shown in this ribbon diagram are the 12–16 inner circle β sheets (inner-pointing arrows) along with adjoining outer circle α helices of NALP14 (**A**, side view; **B**, top view), MATER (**C**), RNH2 (**D**), and porcine RI (**E**). A horseshoe configuration was observed in all cases. The projection was generated computationally by the 3D PDB viewer software.

antigenic determinant of autoimmune oophoritis, inherent to neonatally thymectomized female mice. Of importance, null female mutants for the *Mater* gene proved sterile, a condition attributable to a failure of early embryonic development beyond the 2-cell stage [21]. As such, MATER must be viewed as a maternal effect gene. Significantly, the MATER protein displayed structural features similar to those of NALP14 inclusive of NACHT domain and LRR domains (Fig. 9, A and B). These latter observations strongly suggest that the MATER protein, along with the NALP14 protein, must be considered a member of the germ cell family of LRR-replete NACHT NTPases.

Protein BLAST analysis of the NALP14 amino acid sequence further disclosed 24% identity with yet another known protein, RNH2 (Fig. 3), uncovered in the course of establishing a spermatogonium-specific transcriptome. The degree of identity between the RNH2 and NALP14 proteins, 982 and 993 residues, respectively, was 29%. Although amplicons corresponding to *Rnh2* transcripts, reported by Wang et al., were detected by RT-PCR in spermatogonia, no amplicons were observable in whole ovarian material [14]. In contrast, our present studies, reliant on in situ hybridization (Fig. 7) and QRT-PCR (Fig. 5), revealed *Rnh2* transcripts to be expressed not only in the testis but also in the ovary; namely, in the oocyte. Although this study failed to detect primordial follicle transcripts corresponding to members of the germ-cell family of LRR-replete NACHT NTPases, previous work suggested a modicum of expression of *Mater* transcripts at the primordial follicular stage [11].

The LRR domain is known as a constituent of the primary structure of numerous proteins of diverse origin. Included in this context are more than 60 known cell surface receptors, cell adhesion molecules, extracellular matrix binding glycoproteins, and enzymes. Based on the variable number of LRR repeats and their level of compliance with the general Kajava formula, the LRR protein family can be subdivided into 6 subfamilies. According to this classification, NALP14, MATER, and RNH2 constitute members of the RI (Ribonuclease Inhibitor)-like LRR subfamily (consensus sequence LxxLxLxxN/CxLxxxxoxxLxxoLxx). RI, the prototypic protein for which this family has been named, constitutes a well-established protein, the crystal structure of which has been solved. The latter reveals the LRRs of RI to consist of alternating β sheets and α helices, thereby giving rise to a superhelix. In that all the strands and helices are arranged in parallel to a common axis, the resultant structure is a nonglobular, horseshoe-shaped molecule with curved parallel sheets lining the inner circumference of the horseshoe, the helices flanking the outer circumference (Fig. 10).

In analyzing the perifertilizational ontogeny of *Nalp14*, *Mater*, and *Rnh2* transcripts (Fig. 5C), note was made of a marked decline between GV-stage and MII-stage oocytes. Such pattern of expression may be compatible with a concurrent decline in the corresponding proteins. Although these transcripts significantly decrease by the MII stage, one cannot exclude the possibility of a post-MII role in the course of fertilization, the conclusion of meiosis, and the initiation of early embryonic development. Further experimentation will be necessary to explain the decrease in transcripts before maturation between 2 and 4 wk.

Recently, additional LRR-containing oocyte-specific genes, collectively known as the oogenesin family, have been described [22]. A striking characteristic of the oogenesin family is the so-called degenerated LRRs, variable in both the length and sequences forming the β strands. No significant alignment could be found between NALP14 and the 4 oogenesin genes.

In attempting to establish the relative phylogenetic significance of NALP14, a search for orthologues was carried out. BLAST analysis failed to disclose a viable orthologue with the genomes of *Drosophila melanogaster*, *Caenorhabditis elegans*, *Fugu rubripes*, and *Ciona intestinalis*. Although no orthologue could be detected in the rat, it is recognized that the relevant genome is incomplete at this time. In that other, previously sequenced genomes are still undergoing revisions, it is difficult to conclude with certainty that NALP14 constitutes a mammalian ''invention,'' and that it may be providing a recently acquired higher function that is not shared with submammalian counterparts. A recent contribution [5] suggested an apparent relative abundance of NACHT NTPases in vertebrates, including the human, as distinct from the more limited rep-

resentation in arthropods (*D. melanogaster*), nematodes (*C. elegans*), plants, fungi, and early-branching eukaryotes. At present, the possibility of an NTPase function for NALP14 and its oocytic relatives remains uncertain. Further, pending functional evaluation of recombinant versions of the proteins under study, it is not possible to distinguish between possible ATPase and GTPase functionality. To date, 2 proteins of the broad NACHT family have been evaluated for their NTPase activity and established as GTPases. Specifically, recombinant versions of the HET-E (NACHT/WD repeats) [23] and the CIITA (NACHT/LRR repeats) [24] proteins have been experimentally shown to display GTPase activity. In that no precedent has been established for ATPase activity in NACHT proteins, it is tempting to speculate that NALP14 and its oocytic relatives may represent additional examples of GTPase functionality. Although the relevance of GTPase activity to the function of the NACHT proteins remains uncertain, it is generally accepted that GTP hydrolysis by mainstream GTPases (e.g., Tu, ras, SRP, etc.) promotes a conformational change in their respective protein, which often leads to dissociation of the protein from its target macromolecular complex (e.g., the ribosome). In other words, the GTPase-GTP complex binds to a partner in a signal transduction pathway to generate an effect, after which time the GTPase-GTP complex dissociates. It is thus possible that similar general proteins are operational in the context of the NACHT protein family.

The current manuscript suggests the existence of a novel family of oocyte-based proteins that share significant structural homology [5, 17], and C-terminal LRR and N-terminal NACHT domains. Although the function of members of the LRR-replete NACHT NTPases remains to be elucidated, it is tempting to speculate that the proteins in question may play a meaningful role in the oocyte and possibly in early preimplantation development. Such speculation is strongly supported by the realization that the ablation of the *Mater* gene, an established maternal effect-gene and a member of the germ cell family of LRR-NACHT NTPases, led to embryonic developmental arrest at the 2-cell stage [21].

ACKNOWLEDGMENTS

We acknowledge the expert technical assistance of Ms. Janine M. Calfo. We extend further thanks to Ms. Charu Ramakrishnan (Northwestern University, Evanston, IL), Ms. Kelley Murphy (Huntsman Cancer Institute, University of Utah School of Medicine) and Ms. Sheryl Tripp (Department of Pathology, University of Utah School of Medicine) for excellent technical assistance. We also acknowledge the contribution of Drs. Jurrien Dean and Holly Davies (National Institute of Child Health and Human Development) for evaluating the possibility of *Nalp14* as a downstream product of FIGα, and that of Dr. Francis G. Whitby. Special thanks to members of the Adashi Laboratory for helpful discussions and suggestions.

REFERENCES

1. Wassarman PM, Josefowicz WJ. Oocyte development in the mouse: an ultrastructural comparison of oocytes isolated at various stages of growth and meiotic competence. J Morphol 1978; 156:209–235.
2. Schultz RM. The molecular foundations of the maternal to zygotic transition in the preimplantation embryo. Hum Reprod Update 2002; 8:323–331.
3. Parrott JA, Skinner MK. Kit-ligand/stem cell factor induces primordial follicle development and initiates folliculogenesis. Endocrinology 1999; 140:4262–4271.
4. Durlinger AL, Gruijters MJ, Kramer P, Karels B, Ingraham HA, Nachtigal MW, Uilenbroek JT, Grootegoed JA, Themmen AP. Anti-Mullerian hormone inhibits initiation of primordial follicle growth in the mouse ovary. Endocrinology 2002; 143:1076–1084.
5. Oktay K, Karlikaya G, Akman O, Ojakian GK, Oktay M. Interaction of extracellular matrix and activin-A in the initiation of follicle growth in the mouse ovary. Biol Reprod 2000; 63:457–461.
6. Damiano JS, Oliveira V, Welsh K, Reed JC. Heterotypic interactions among NACHT domains: implications for regulation of innate immune responses. Biochem J 2004; 381:213–219.
7. Koonin EV, Aravind L. The NACHT family—a new group of predicted NTPases implicated in apoptosis and MHC transcription activation. Trends Biochem Sci 2000; 25:223–224.
8. Bondy CA, ZJ, Lee WH. Chapter 13. In: lora De Pable CGS, Weintraub BD (eds.), *Handbook of Endocrine Research.* San Diego: Academic Press; 1993:265–286.
9. Breathnach R, Chambon P. Organization and expression of eucaryotic split genes coding for proteins. Annu Rev Biochem 1981; 50:349–383.
10. Hamatani T, Falco G, Carter MG, Akutsu H, Stagg CA, Sharov AA, Dudekula DB. Age-associated alteration of gene expression patterns in mouse oocytes. Hum Mol Genet 2004; 13:2263–2278.Epub 2004 Aug. 18.
11. Tong ZB, Nelson LM. A mouse gene encoding an oocyte antigen associated with autoimmune premature ovarian failure. Endocrinology 1999; 140:3720–3726.
12. Tong ZB, Nelson LM, Dean J. Mater encodes a maternal protein in mice with a leucine-rich repeat domain homologous to porcine ribonuclease inhibitor. Mamm Genome 2000; 11:281–287.
13. Hofsteenge J, Kieffer B, Matthies R, Hemmings BA, Stone SR. Amino acid sequence of the ribonuclease inhibitor from porcine liver reveals the presence of leucine-rich repeats. Biochemistry 1988; 27: 8537–8544.
14. Wang PJ, McCarrey JR, Yang F, Page DC. An abundance of X-linked genes expressed in spermatogonia. Nat Genet 2001; 27:422–426.
15. Kajava AV. Structural diversity of leucine-rich repeat proteins. J Mol Biol 1998; 277:519–527.
16. Kobe B, Deisenhofer J. Crystallization and preliminary X-ray analysis of porcine ribonuclease inhibitor, a protein with leucine-rich repeats. J Mol Biol 1993; 231:137–140.
17. Koonin EV, Aravind L. Origin and evolution of eukaryotic apoptosis: the bacterial connection. Cell Death Differ 2002; 9:394–404.
18. Saraste M, Sibbald PR, Wittinghofer A. The P-loop—a common motif in ATP- and GTP-binding proteins. Trends Biochem Sci 1990; 15: 430–434.
19. Walker JE, Saraste M, Runswick MJ, Gay NJ. Distantly related sequences in the alpha- and beta-subunits of ATP synthase, myosin, kinases and other ATP-requiring enzymes and a common nucleotide binding fold. Embo J 1982; 1:945–951.
20. Bertin J, Nir WJ, Fischer CM, Tayber OV, Errada PR, Grant JR, Keilty JJ, Gosselin ML, Robison KE, Wong GH, Glucksmann MA, DiStefano PS. Human CARD4 protein is a novel CED-4/Apaf-1 cell death family member that activates NF-kappaB. J Biol Chem 1999; 274:12955–12958.
21. Tong ZB, Gold L, Pfeifer KE, Dorward H, Lee E, Bondy CA, Dean J, Nelson LM. Mater, a maternal effect gene required for early embryonic development in mice. Nat Genet 2000; 26:267–268.
22. Dade S, Callebaut I, Mermillod P, Monget P. Identification of a new expanding family of genes characterized by atypical LRR domains. Localization of a cluster preferentially expressed in oocyte. FEBS Lett 2003; 555:533–538.
23. Espagne E, Balhadere P, Begueret J, Turcq B. Reactivity in vegetative incompatibility of the HET-E protein of the fungus *Podospora anserina* is dependent on GTP-binding activity and a WD40 repeated domain. Mol Gen Genet 1997; 256:620–627.
24. Raval A, Weissman JD, Howcroft TK, Singer DS. The GTP-binding domain of class II transactivator regulates its nuclear export. J Immunol 2003; 170:922–930.